

Chapter

Current Development of Automotive Powertrain Components for Low Friction and Wear Reduction through Coating and Heat Treatment Technology

Sung Chul Cha, Kyoung Il Moon and Hae Won Yoon

Abstract

Recent findings of R&D for powertrain components concerning friction and wear reduction are described in this chapter. These are realized through lubrication technology of coating and heat treatment, which are fit for this book. In the first part, nano-complex coatings for parts of future mobility are presented with their friction and wear behavior. The application of an alloying target was proposed to promote the commercial use of nanocomposite coatings. In the second part, the importance on pre-treatments-related silicon oxide-diamond-like carbon (SiO-DLC) coating for the smallest part of fuel system is described. The optimization of cleaning for the balls before coating was resulted: The best cleaning performance presented the addition of acetone cleaning, water boiling, and then acetone cleaning, confirmed by fluorescence analyzers. The third part of this work was developing low-temperature vacuum carburizing and pre-treatment for parts of injector, stopper (SUS303), and position ring (1.4305) with high wear resistance. The difference between two steels led to the result: high molybdenum of 1.4305 formed Mo-oxides on the surface during acid etching. These Mo-oxides resolved quickly by hydrogen during carburizing and then enabled activated carburizing. The 1.4305 was appropriate for the carburizing and was chosen for stopper.

Keywords: ultralow friction Zr-based coating, nano-complex coating, low friction hard coating, SiO-DLC, coating's pre-treatment, low-temperature vacuum carburizing

1. Introduction

1.1 Increasing demands on multifunctional nanocomposite coatings

Recently, the industry demands the right property in the right place (application). It is well known the life span of the machinery could be increased and the new properties could be endowed through the application of proper coating systems. Therefore, attempts have been made to develop various coatings with properties suitable for mechanical parts in different applications. For example, a Swiss coating company, Plaitit, has developed over 100 various coating systems in order to get optimal performance according to the working functions of the tools and machine components [1]. In addition, a German bearing company, Schaeffler, has developed the customized surface technology in which the different coatings are designed for the different bearing systems and this resulted in the increased lifetime, increased functionality, and other added value to the systems [2]. Furthermore, the industry demands new coating systems with very different or opposite properties for the superior properties of the product. For instance, the new coating systems exhibit high hardness and low friction, or high conductivity and high corrosion resistance. To obtain such opposite properties in a single coating system, two or more phases of the coating material must be formed in the nanometer-scale area which is a nanocomposite coating. Therefore, new demands for nanocomposite coatings are gradually increasing.

As shown in **Figure 1**, nanocomposite coating can be divided into two types, hard matrix nanocomposite coating and soft matrix nanocomposite coating, depending on the matrix material. If the nanocomposite coatings could be formed by the combination of ceramic phases, such as nitrides and carbides, higher hardness, higher thermal stability, and the corrosion and oxidation resistance could be obtained. The properties are very useful for molds and tools. Up to the early twenty-first century, most of the commercialized nanocomposite coatings were made by a combination of ceramic phases. As a result, coatings with the super-hardness over 40 GPa, the ultra-hardness over 70 GPa, and thermal stability over 1100°C had been developed [3, 4]. The crystalline phase of the nanocomposite coating is nitride, carbide, boride, and oxide, and the amorphous phase may be metal or ceramic. In such a case, the properties of the

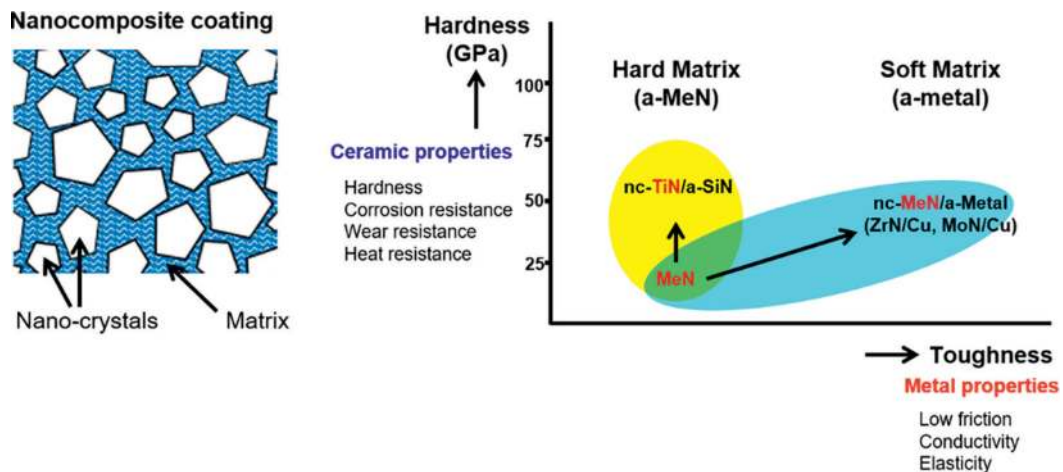


Figure 1. Two kinds of nanocomposite coatings are based on the matrix materials: Hard matrix and soft matrix.

metal phases, such as high toughness, electric conductivity, and low friction, could be obtained with the properties of ceramic phases. Because of the wider spectrum of properties, including opposite properties, the soft matrix coatings could be used in various industrial fields.

In the early twenty-first century, a diamond-like carbon (DLC) coating has been used as a protective coating for various parts of the automobile engine. The engine performance has been greatly improved by adopting the low friction and high durable coating. But automobile companies tried to adopt the new modified engine oils for better lubrication where the various additives are designed to have protective effects on the steel surfaces. But such additives have no compatibility with non-metallic coating and even they could damage DLC coatings [5]. Also the future demands on the internal combustion engine (ICE) systems and the application conditions of the mobility parts for the electric vehicles (EV) are much severe and worse. Future mobility shall be operated under non-lubrication conditions, which lead to more severe conditions for friction and wear of components. Consequently, new coating systems should be developed to have the better capability with the future automobile systems. Nanocomposite coating can be applied to future mobility parts.

1.2 Preparation of the alloying targets for nanocomposite coatings

The design rules for the nanocomposite coatings are discussed in the previous manuscripts [6, 7] but the most important basic rule is two elements are needed and they should be immiscible or low miscible properly each other [8]. Therefore, it is not easy to manufacture an alloying target made of an element that meets the requirements for depositing a nanocomposite coating by a general conventional target manufacturing method. The most commonly used method for the fabrication of a nanocomposite coating is a multi-cathode sputtering system that uses as many targets as additional elements [9]. However, in order to deposit a nanocomposite coating of a desired composition, it is necessary to control element targets having different sputtering yields to an appropriate power level, and to obtain a uniform coating, it is necessary to control various process parameters [10]. These complex equipment and process conditions hinder the mass production of nanocomposite coatings. In this study, an alloying target with high chemical homogeneity, high structural uniformity, and excellent mechanical properties was developed for the mass production of nanocomposite coatings.

The alloying target could be prepared generally by the preparation of the alloying powders and the subsequent sintering of the alloying powders, which is indexed as a red line in **Figure 2**. Because the alloying rules for nanocomposite materials are the same for the amorphous materials [11], the first attempts were made to find the proper alloys among amorphous materials and the target making procedures for the alloy systems with the amorphous compositions, such as Zr-Cu and Ti-Cu based alloys, summarized in **Figure 2** and it was detailed explained by Moon et al. [6]. Theoretically, if the amorphous alloys with high glass-forming ability (GFA), they could be made as the bulk targets by the casting process. According to our previous study, only one case was successful in Zr-Cu-Si system in which the target with a diameter of 127 mm (5 inches) was successfully prepared by a casting process [12]. Since the amorphous materials have been developed with the GFA of the size around 1–2 mm [13], the larger size targets should be prepared by a two-step process; firstly, the alloying powders are prepared by atomization, and then they are consolidated by the proper sintering processes. If the alloying powders could not be prepared by an atomization process as in Mo-Cu [14], Ti-Al [15], and Al-Cr based systems, the proper

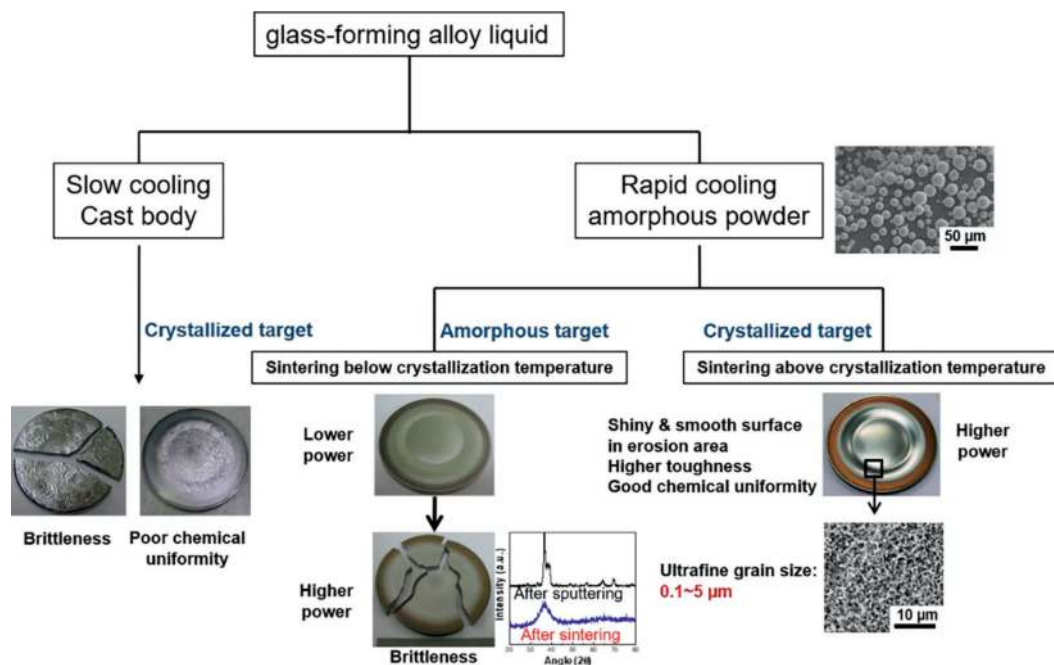


Figure 2.
Summary of the fabrication of alloying sputtering targets [6].

ball milling processes were used to prepare the alloying powders. Subsequently, the bulk targets could be made by various sintering processes, such as vacuum hot press (VHP), spark plasma sintering (SPS), hot isostatic pressing (HIP), and so on. The targets could be used without trouble during the sputtering process only when they were consolidated to some specific microstructures with sufficient high toughness [6].

1.3 Properties of the nanocomposite coatings prepared with single alloying targets

Since the alloying targets for the nanocomposite coatings are made with amorphous materials, an amorphous phase could easily be formed during the sputtering process, **Figure 3**. According to our previous studies [6, 7], rather to get the nanocomposite structure, the sputtering parameters should be carefully selected, such as a high level of sputtering power, high N_2 : Ar gas mixing ratio, and a high process temperature. An amorphous coating was easily formed when nonreactive sputtering of an alloying target in an Ar gas atmosphere. On the other hand, when reactive sputtering was performed on the same alloying target in an Ar- N_2 mixed gas atmosphere, a nanocomposite nitride phase was formed. The amorphous phase coating shows a higher enough toughness to be used as a buffer layer for the hard coatings [16]. Also, since the amorphous coating shows high corrosion protection with high conductivity, it could be used as the coating for the bipolar plate in the fuel cell [17]. The nanocomposite nitride coatings showed high hardness around 20–30 GPa, and according to the data on the coatings from the various amorphous targets with different metal contents, the hardness of the nitride nanocomposite coatings increased linearly with the decreases in the soft-metal content [6]. The nitride coatings showed very low friction properties even compared with DLC coating in the boundary lubrication conditions of the modified oils. Therefore, it could be used in the various applications of ICE and EV systems.

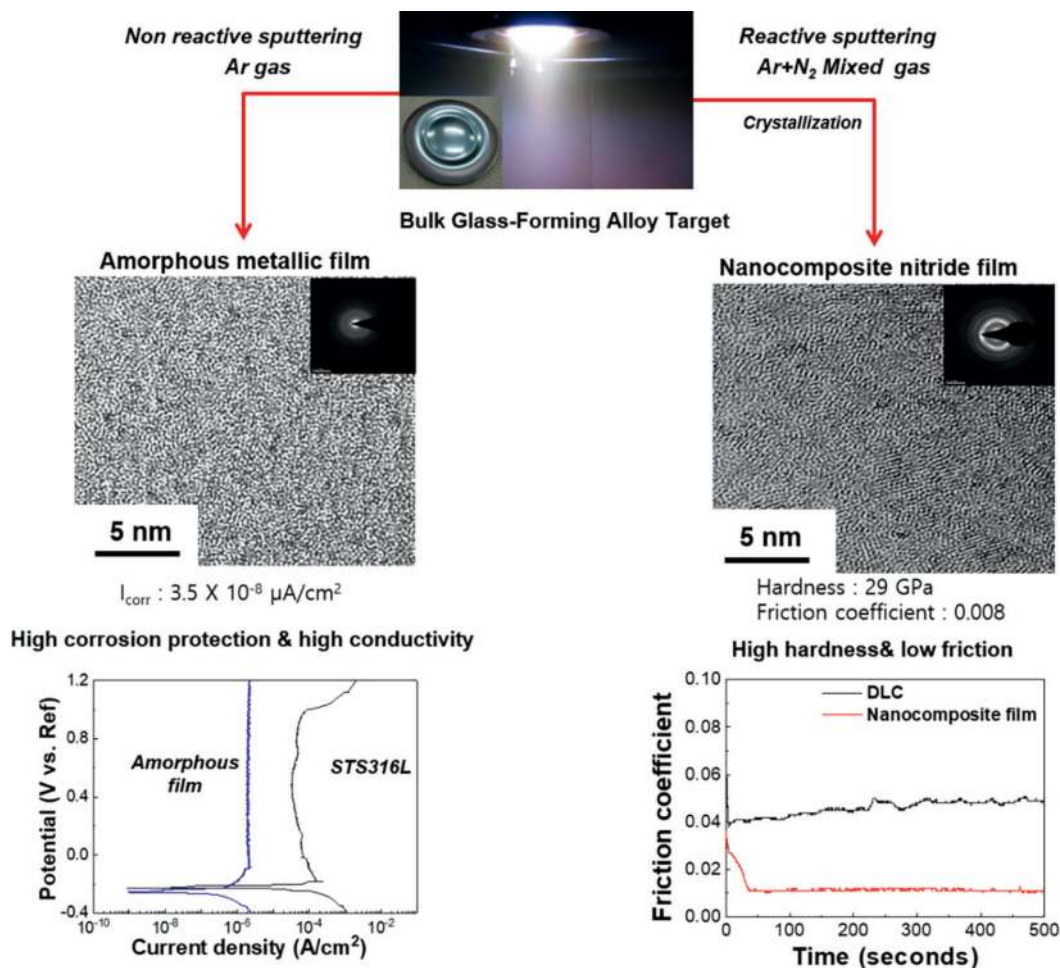


Figure 3. Summary of the properties of the coatings prepared with the Zr-Cu-Al-Mo alloying targets.

Erdemir et al. [18] reported that MoN-Cu coatings showed a better friction coefficient in the boundary lubrication area of basic oil and the existence of a Cu matrix could formulate the formation of easy shear tribofilms. In our studies [19, 20], it is also found that low friction and high durable tribofilms were easily formed after wear tests. According to the investigations by RAMAN and XPS, the tribofilms were considered to be amorphous carbon films that must be formed from the decomposition of engine oils by the catalytic effects of the Cu matrix. The more severe the test conditions resulted in the thicker tribofilms [18]. After the engine ring-liner scuffing test of ZrCuSiN, the tribofilms were formed on the surface of the engine ring and the thickness was about 500–700 nm as shown in **Figure 4**. Since the thick tribofilms had high hardness and low friction properties, they could prevent the surface of the engine parts effectively even in severe wear conditions.

The most important result from the studies with the alloying targets is that the composition of the coating layer was almost the same as that of alloying target according to electron-probe microanalysis (EPMA) data on the surface area and glow-discharge optical-emission spectroscopy (GDOES) data throughout the thick coating layer [6]. In particular, for coatings deposited by microcrystalline targets, excellent composition uniformity between the target and the coating is achieved [6, 11]. These

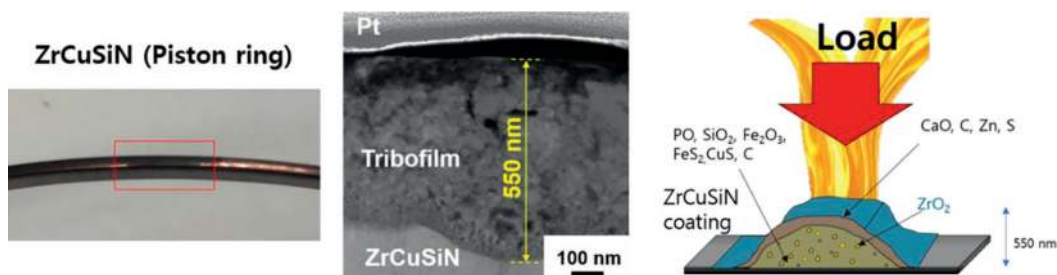


Figure 4. TEM investigation on the cross-section of tribofilms after engine ring-liner scuffing test [19].

results suggest that using an alloying target with uniform composition and fine microstructure is a convenient method to reduce process cost and deposit the designed composition.

2. Importance of pre-treatments of coating to use the smallest spherical parts of powertrain fuel systems

Complex coating technique for the smallest spherical parts (balls, 2–4 mm diameter) of the modern fuel injector is detailed reported by Cha et al. [21]. The fuel injector is responsible for the precise fuel proportioning related to controlled combustion and reduced emissions. Materials of fuel injector have to possess high resistances to high pressure of 200–1000 bar, high temperature, and severe corrosive media related fuels. During injector operation coated ball, which is welded to the needle, moves up and down and contacts with the valve seat to open and close the fuel injection holes. Hence, defects in sealing and contacting surfaces lead to problems like leakage. The material of the ball is SUS440C stainless steel with a hardness of HV 670–700. The coating consists of three layers, Cr as the bonding layer on the substrate, WC as the buffer layer on Cr, and SiO-DLC as the functional top layer. To coat the balls and to maximize the production amount, the rear magnet fixing method was applied. Only 80% of the ball is coated, and the uncoated area of 20% is welded with a needle. The combination of physical vapor deposition (PVD) and plasma-assisted chemical vapor deposition (PACVD) coating process and proper jig led to the coating thickness of 1.8–2.17 μm , the coating hardness of 22.2–25.7 GPa, and the coating adhesion of 35 N. This work aims to achieve quality improvements through the optimization of coating pre-treatments, that is, cleaning of the balls before coating. The residue-free cleaning of the balls has utmost importance for coating processes, that is, without a residue-free surface, the coating can fail or be rejected.

Hundreds of balls from the ball manufacturer are supplied in plastic bags with rust-preventing lubricant oil. The process steps at a coating company are ball arrival, cleaning, drying, jig mounting, coating, demounting, thermoshock testing, inspection, and delivery to the assembling company. Before PVD and PACVD coating, the balls are oil-free washed, dried, and then mounted on a coating jig using the rear magnet fixing method in a vertical direction in the coating machine. The defects of coating can be divided into three sorts: material fault (stab, dent, and scratch), cleaning fault (coating spallation caused by residual oil), and coating fault (spallation caused by foreign particles and coating particles). The defects that occurred from ball cleaning and coating are spallation of coating, particles, surface defects, rainbow, and waves of the border area between coated and uncoated zone, **Figure 5**.

The current cleaning process is composed of three-times-cleaning, five-times-rinsing and two-times-drying. And the sequence is 1st cleaning- 1st rinsing- 2nd cleaning- 2nd rinsing- 3rd cleaning- 3rd, 4th, 5th rinsing- N₂ drying and finally vacuum drying. First cleaning detergents are a mix of amine, alcohol, hydrocarbon and acid, whereas 2nd cleaning is alcohol and amine, in the third cleaning alcohol and hydrocarbon are combined. Rinsing is carried out at 40°C in an ultrasonic bath and vacuum drying at 80°C. In total, 30 % of total coating defects can be avoided by optimizing the cleaning procedures. Therefore, the defects of cleaning shall be revised.

Several trials as revision are conducted: ① the reduction of cleaning amount, ② the addition of up-and-down-movement during cleaning, ③ spraying, ④ gauze washing,

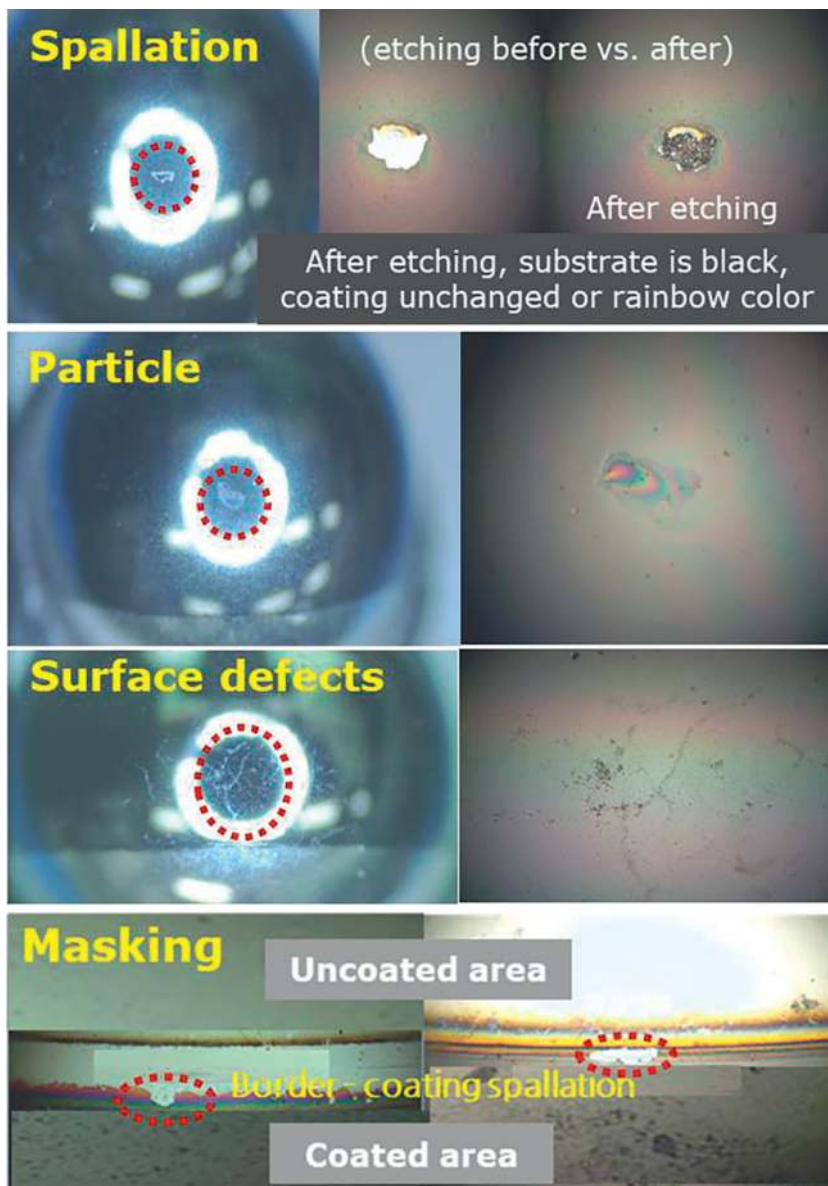


Figure 5. Coating and cleaning defects: Spallation, particle, surface defect and masking (left: Microscope, right: Optical microscope (200x)).

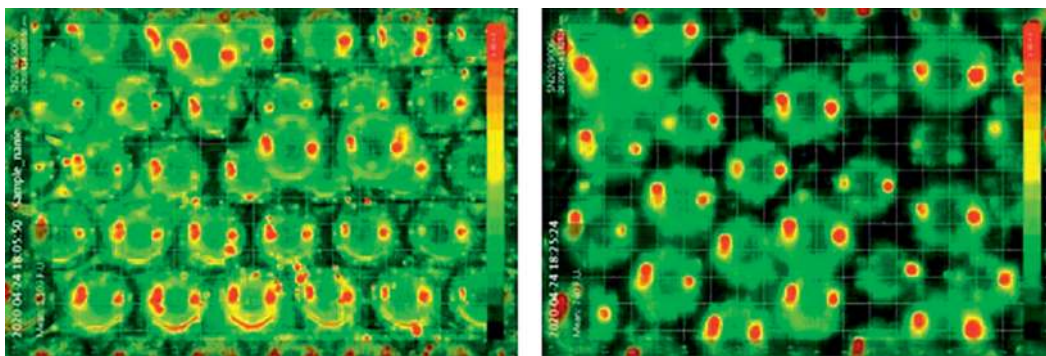


Figure 6. Results of Recognoil @2 W-current (left) vs. revised cleaning (right). Red color is oil residue.

③ the change of cleaning conditions (detergent concentration, temperature, and duration), ⑥ the cleaning of ultrasonic bath in acetone, ⑦ the boiling, and ⑧ the acid etching. These are compared with measurement of corrosion test on metal surfaces and of total organic carbon, but not representative both for the testing by massive amounts and mass production.

Especially, the evaluation through fluorescence analyzers, for example, CleanoSpector by Sita Co., Germany [22] and Recognoil by TechTest Co., Czech Republic [23], can clarify the effects of cleanliness. CleanoSpector measured relative fluorescence unit for current cleaning 4, for revised process 1.7 (additional pre-treatment to current process, i.e., the addition of acetone cleaning in ultrasonic bath, de-ionized (DI) water boiling and acetone cleaning in ultrasonic bath), and for non-washed ball 415–598. Recognoil @2 W can measure fluorescence intensity and show as image: fluorescence intensity for current cleaning 1.103 and for revised process 740 and for non-washed ball 2.000.000. **Figure 6** shows images of fluorescence detector Recognoil @2 W-current cleaning (left) vs. revised cleaning (right), and the red color is oil residue. Both analyzers showed excellent measuring and detecting performance. As a main result, the best cleaning performance showed the addition of acetone cleaning in ultrasonic bath, DI water boiling and again acetone cleaning in ultrasonic bath.

In summary, the quality of coated balls is essentially achieved through cleaning before coating. The retained residue on the cleaned ball surface causes the defects like spallation of coating, particles, surface defects, rainbow, and waves of the border area between coated and uncoated zone. From many conducted trials and measuring methods, the addition of acetone cleaning in the ultrasonic bath, DI water boiling, and acetone cleaning showed high effective cleaning method. And the evaluation through fluorescence analyzers enabled excellent measuring and detecting performance, in contrast, the measurements of corrosion test on metal surfaces and of total organic carbon were not applicable.

3. Effects of molybdenum on hardening properties of stainless steels by low temperature vacuum carburizing and pre-treatment

Recent CO₂ regulations for light-duty passenger cars, especially in Europe, decreases from 130 g/km (2015), 95 (2021), 80 (2025) to 59.4 (2030) [24].

Automakers endeavor to improve powertrain design for fuel efficiency and satisfy emissions requirements. The fuel injector is the main component of precise fuel metering to control combustion characteristics and reduce emissions. Currently, fuel injectors are developed with higher pressures to meet the CO₂ regulation and get competitiveness. The injector is composed of the coil and the needle assembly, which has a stopper, armature, position ring, needle bar, and ball. Materials of injector shall have resistances for high pressure, high temperature, corrosion, and abrasion. The stopper and position ring are continuously impacted by the vertical motion of adjacent parts during operation and are currently applying expensive carburizing heat treatment [21, 25, 26]. Thus, it is necessary to develop a cost-effective heat treatment. New developed carburizing has a marginally different hardening principle from conventional carburizing methods. The structure of current carburized austenitic stainless steel is that carbon is dissolved in the metal matrix to increase the surface hardness caused by high compressive stresses, whereas there is no carbide formation to worsen the corrosion resistance [27] and weldability. Concerning expanded austenite structure, that is, S-phase, nitrogen atoms diffused into the face-centered cubic (fcc) lattice at low temperature, and the S-phase containing layer has high corrosion resistance and high surface hardness [28, 29]. The objectives of this work were to develop low-temperature vacuum carburizing and their acid etching of stainless steels for modern injector parts.

As experimental and results, the concerned parts were stopper (SUS303, 0.05 C-0.3 Si-1.9 Mn-0.03 P-0.32 S-17.2 Cr-8.5 Ni-0.25 wt% Mo) and position ring (1.4305, 0.05 C-0.3 Si-1.9 Mn-0.03 P-0.31 S-17.6 Cr-8.6 Ni-0.4 Cu-0.4 wt% Mo), which made by stainless steel containing 2 wt% Mn for machinability. At first, currently applied parts were measured, carburized layer thickness of 21.3–24.1 μm and hardness HV_{0.05} 914–959.

To substitute the current low-temperature gas carburizing process, new low-temperature vacuum carburizing, and acid etching pre-treatment were developed to reduce the cost and improve product quality.

Stainless steels with more than 12 wt% chromium have Cr₂O₃ passivation layer with corrosion resistance, but this layer plays as a barrier layer for carburizing. The pre-treatments for deletion of passive layer, for example, acid etching, NH₄Cl, plasma, and halogen gas, are necessary. Acid etching was chosen and it was to find their optimal condition, for example, acid media, concentration, and duration. Moreover, the objective was to avoid the formed soot during carburizing. Soot causes failure at laser welding with the formation of pores and the reduction of corrosion resistance [30]. In this work, low-temperature vacuum carburizing was performed in a commercial vacuum carburizing furnace (VH556–10, Rübige, Austria). High purity acetylene (C₂H₂, 99.90%) and hydrogen (H₂, 99.999%) were used as the process gases. Low-temperature vacuum carburizing was carried out for 24 h (including heating and cooling times) with a carburizing potential (Kc) of 0.32 at a working pressure of 800 Pa and a temperature of 450°C. Process conditions were partly used as reported in previous work [25, 26], and further optimized.

Especially, SUS303 and 1.4305 showed different pitting and oxide regeneration behavior by acid etching regarding the chemical composition difference: Stopper (SUS303) and position ring (1.4305) were tested with the variation of acid concentration and duration. As a result, the position ring (1.4305) had lower pitting than that of the stopper (SUS303) and showed carburizing behavior. From diverse acid concentrations (high/middle/low) in nitric-hydrofluoric acid, the mid concentration

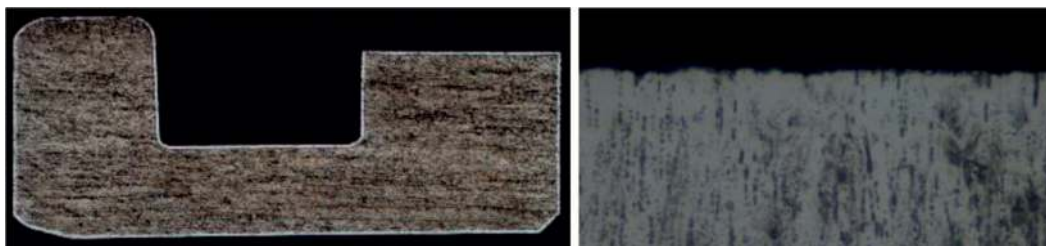


Figure 7. Carburized stopper (SUS303) as cross section (50x, left) and surface layer (500x, right) (mid acid etching of pH 1.67).

of pH 1.67 and short time of 55 seconds had no pitting and enabled carburizing on all surfaces with the hardness of $HV_{0.05}$ 902–942, **Figure 7**.

In the case of stopper SUS303, when the acid etching time was short, the carburized layer was not formed. Oppositely, if the time was increased beyond a certain level, the carburized layer was formed, but its hardness had a low value between $HV_{0.05}$ 500 and 600, the reason was that MnS inclusions at the surface led to severe MnS pitting over time. However, in 1.4305 material, at the same time as the above-mentioned acid etching was performed, not only the pitting was disabled, but also the carburized layer was completely formed on the surface.

As a result of application to the product, the position ring (1.4305) had lower pitting and homogenous carburized thickness and hardness than those of the stopper (SUS303) under the same acid condition, **Figure 8**. For a detailed declaration of this reason, the number, average size, and composition fraction of MnS inclusions were analyzed by optical microscope (OM) and scanning electron microscope-energy-dispersive X-ray spectroscopy (SEM-EDX). The surface before and after acid etching was analyzed by X-ray photoelectron spectroscopy (XPS). OM Image analyzer resulted from position ring (1.4305) had more and bigger MnS inclusions in position ring than those of stopper. EDX mapping confirmed that Mn, S distribution at stopper and position ring had no significant differences. However, the difference in chemical composition, especially, molybdenum, was shown.

One of the reasons for different pitting behavior was the different Mo content and related pitting resistance equivalent number (PREN) (position ring: 1.4305, 0.4 wt% Mo, stopper: SUS303, and 0.25 wt%). To investigate other reasons, the Mo and Mo-oxide contents of both steels before and after acid etching were analyzed by XPS in-depth, **Table 1** and **Figure 9**. There was no difference before etching, but after etching there was a significant change in Mo and Mo-oxide composition in depth. And Mo of the position ring (1.4305) was higher at the surface and in-depth as well, **Figure 9**. In detail, the composition of formed oxide layers at the position ring and stopper were different. Position ring had MoO_2 , MoO_3 at the surface, and Mo, MoO_2 , and MoO_3 in-depth were higher than those of the stopper. Thus, high Mo content led to high pitting resistance, and the formation of a fast Mo-oxide layer because of higher Gibbs free energy than Cr_2O_3 [31].

The relatively high content of molybdenum in the 1.4305 steel formed Mo-oxides on the surface during acid etching, which the excessive pitting by the MnS inclusion site was prevented. Furthermore, these oxides (mainly MoO_3) resolved easily by hydrogen during low-temperature vacuum carburizing and subsequently enabled activated carburizing [32].

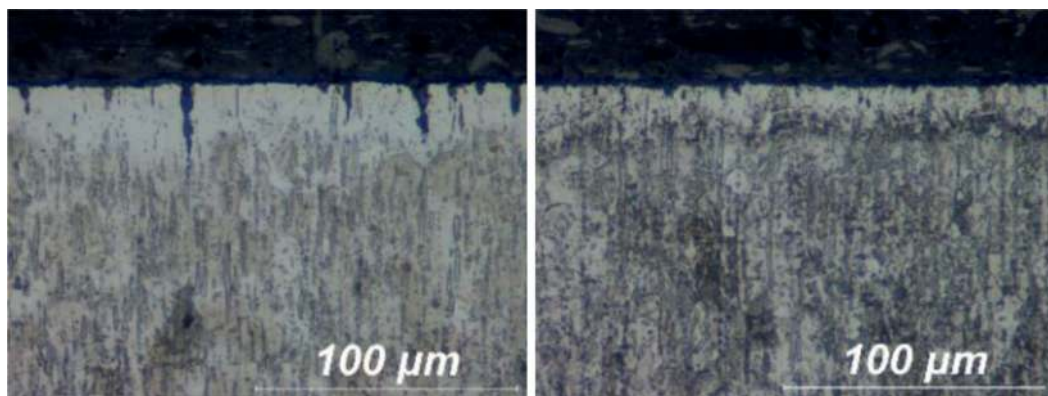


Figure 8. Difference of pitting of carburized layer under same acid condition (left: Stopper (SUS303), right: Position ring (1.4305)).

XPS results (at%)		1 nm	8 nm	17 nm
Stopper (SUS303)	Mo	64.85	62.06	64.04
	MoO ₂	30.20	32.61	32.33
	MoO ₃	4.95	5.33	3.63
Position ring (1.4305)	Mo	36.64	69.16	79.11
	MoO ₂	45.48	25.8	13.27
	MoO ₃	17.88	5.04	7.63

Table 1. XPS results from surface to depth of stopper (SUS303) and position ring (1.4305).

In conclusion, 1.4305 showed outstanding carburizing properties, hardness of HV_{0.05} 911–1059, the thickness of 20–25 μm, including satisfaction of weldability and low roughness of Rz 0.809 μm, **Figure 10**. In final, stopper material was changed to position ring material 1.4305, and subsequently the test for mass production is carried out.

In summary, the objectives of this work were to develop low-temperature vacuum carburizing and their acid etching for injector parts, which were stopper (SUS303) and position ring (1.4305). Currently applied parts had the carburized thickness of 21.3–24.1 μm and the hardness of HV_{0.05} 914–959. The new carburizing and acid etching should enhance the hardness-related wear resistance and durability, the reduction of production cost, and product quality. As an experimental result, SUS303 and 1.4305 showed different pitting and oxide regeneration behavior by acid etching due to the material composition difference. In SUS303, when the acid etching time was short, the carburized layer was not formed. If the time was increased, the carburized layer was formed, but its hardness was low, the reason is that MnS inclusions at the surface led to severe MnS pitting. In 1.4305, at the same time as the acid etching pre-treatment was performed, not only the pitting was suppressed, but the carburized layer was completely formed on the surface. The relatively high content of molybdenum in 1.4305 formed Mo-oxides on the surface during acid etching, which the excessive pitting by the MnS inclusion site was prevented. Furthermore, these oxides (mainly MoO₃) were resolved

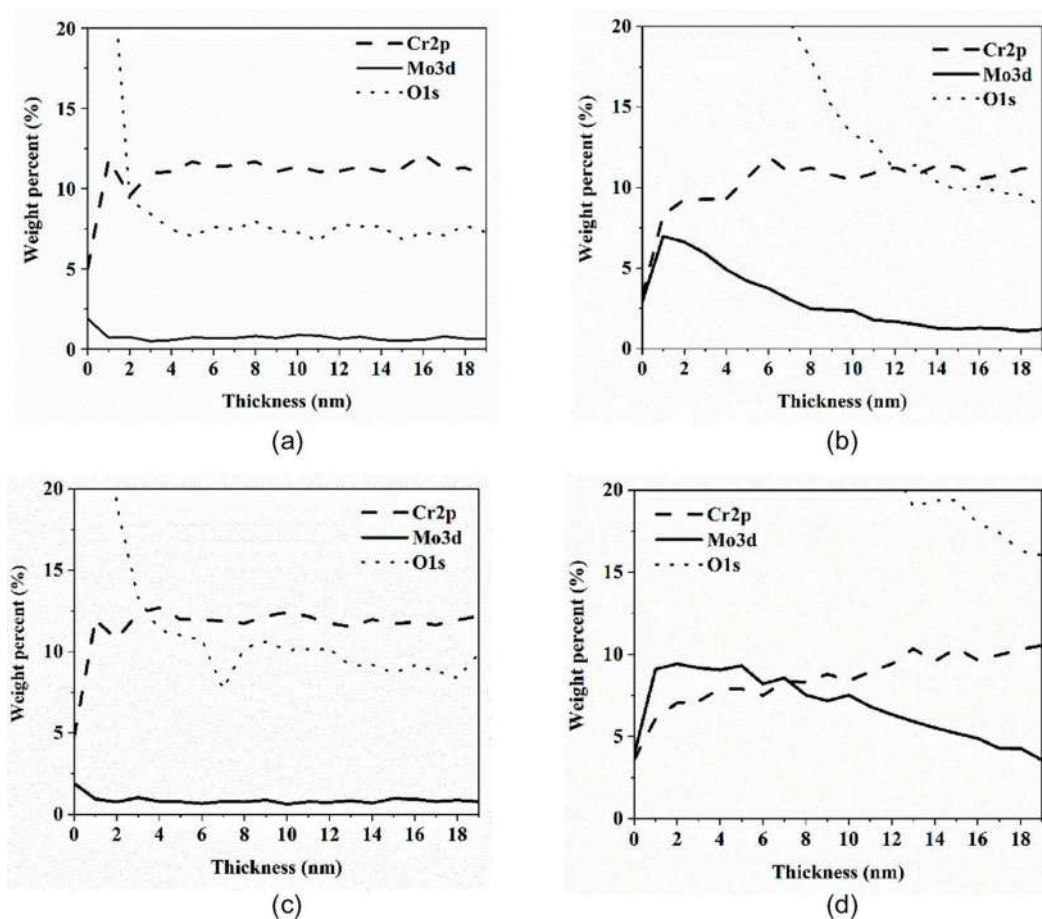


Figure 9. XPS comparison of each element (Cr, Mo, O) in weight percent (stopper vs. position ring). a) Stopper initial. b) Stopper after acid etching. c) Position ring initial. d) Position ring after acid etching.

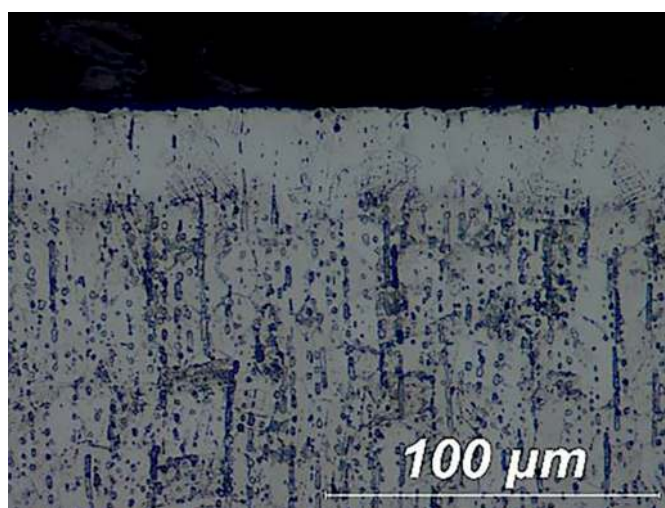


Figure 10. Developed pre-treated and carburized layer on position ring (1.4305).

easily by hydrogen during carburizing and subsequently enabled activated carburizing [32]. In conclusion, 1.4305 showed excellent carburizing properties: hardness of HV_{0.05} 911–1059, thickness of 20–25 μm, satisfaction of weldability, and low roughness. Therefore, the stopper material was changed to position ring material 1.4305.

4. Conclusions

From our previous studies on various coating systems [6, 7, 14, 15, 17, 19, 20], the mass production of a nanocomposite coating could be easily possible by using a single alloying target. Furthermore, it is considered that the nanocomposite coating could be prepared with the different phases that possess the desired properties by designing the composition of the alloying target and controlling the conditions of the coating process. Now, it has been tried to develop new coating systems suitable for harsh environments, such as non-lubrication conditions and heavy-loading conditions. Also, the mechanism for the catalytic effects of Cu has not been revealed at all and the effective amount and structure of Cu in the coating should have been studied. It will be discussed in other manuscripts. As advanced surface lubrication, the nanocomposite coatings can substitute the current applied coatings, for example, DLC, SiO-DLC, and ta-C, in near future. With the consideration of economic aspects and reality, coating and heat treatment technology for automotive powertrain components have been developed for low friction and wear reduction. Concerning coating technology injector balls are SiO-DLC coated with PVD and PACVD and proper jig for low friction and wear. For the achievement of coating quality, pre-treatment of coating, and cleaning is essential. Therefore, the improvement of cleaning for the balls was done: the most effective cleaning was the pre-treatment of acetone cleaning in the ultrasonic bath, DI water boiling, and acetone cleaning in ultrasonic bath before the current cleaning process. In particular, the fluorescence analyzers clearly clarified the cleanliness level. Concerning heat treatment technology, low-temperature vacuum carburizing and pre-treatment for injector parts were developed and showed during acid etching Mo-oxides on the surface are formed, especially by 1.4305 with high molybdenum content. Through these Mo-oxides with easy resolution behavior, carburizing was promoted. The changed stopper steel (1.4305) was appropriate for the new vacuum carburizing and their acid etching.

Acknowledgements

This study has been conducted with the support of the Korea Institute of Industrial Technology as “Development of intelligent root technology with add-on modules” (KITECH EO-22-0005).

The work “Importance on pre-treatment of coating for using the smallest spherical parts of powertrain fuel systems” was carried out with the collaboration of coating company DONGWOO HST.

The part “Effects of molybdenum on hardening properties of stainless steels by low-temperature vacuum carburizing and pre-treatment” was conducted with institutions

and companies (KITECH, Dongwoo HST, Samlak). Especially, Dr. Jun-Ho Kim from KITECH is truly appreciated for his collaboration.

Notes

The work “Effects of molybdenum on hardening properties of stainless steels by low-temperature vacuum carburizing and pre-treatment” was orally presented at the session “vacuum processes and technology” in the 31st ASM Heat Treating Society Conference (Heat Treat 2021). The expanded abstract was published (DOI: 10.31399/asm.cp.ht2021exabp0107, ASM permitted for this reuse).

Nomenclature

a	Amorphous
a-MeN	Amorphous metal-nitride
DI	Deionized
DLC	Diamond-like carbon
EPMA	Electron probe microanalyzer
EV	Electric vehicle
fcc	Face-centered cubic
GDOES	Glow-discharge optical emission spectroscopy
GFA	Glass-forming ability
HIP	Hot isostatic pressing
HV	Vickers hardness
ICE	Internal combustion engine
Kc	Carburizing potential
nc	Nanocomposite
OM	Optical microscope
PACVD	Plasma-assisted chemical vapor deposition
PREN	Pitting resistance equivalent number
PVD	Physical vapor deposition
RAMAN	Raman spectroscopy
Rz	Ten-point mean roughness
SEM-EDX	Scanning electron microscope-energy-dispersive X-ray spectroscopy
SiO-DLC	Silicon oxide-diamond-like carbon
SPS	Spark plasma sintering
ta-C	Tetrahedral amorphous carbon
TEM	Transmission electron microscopy
VHP	Vacuum hot press
XPS	X-ray photoelectron spectroscopy

Author details


Sung Chul Cha^{1*}, Kyoung Il Moon² and Hae Won Yoon²

1 Hyundai Motor Group-Hyundai Kefico, Gunpo, Gyunggi, Republic of Korea

2 Korea Institute of Industrial Technology, Siheung, Gyunggi, Republic of Korea

*Address all correspondence to: sungchul.cha@hyundai-kefico.com

IntechOpen

© 2022 The Author(s). Licensee IntechOpen. This chapter is distributed under the terms of the Creative Commons Attribution License (<http://creativecommons.org/licenses/by/3.0>), which permits unrestricted use, distribution, and reproduction in any medium, provided the original work is properly cited. 

References

- [1] Platit. Compendium [Internet]. Available online: https://www.platit.com/media/filer/2022/pl2022-01_compendium_en_web_druckbogen.pdf
- [2] Schaeffler. Coating Solutions from Schaeffler [Internet]. Available online: <https://www.schaeffler.com/en/innovation/technology/technology.jsp>
- [3] Musil J. Hard and superhard nanocomposite coatings. *Surface and Coatings Technology*. 2000;123(1-3):322-330. DOI: 10.1016/S0257-8972(99)00586-1
- [4] Voevodin A, Zabinski J. Nanocomposite and nanostructured tribological materials for space applications. *Composites Science and Technology*. 2005;65(5):741-748. DOI: 10.1016/j.compscitech.2004.10.008
- [5] Kosarieh S, Morina A, Laine E, Flemming J, Neville A. The effect of MoDTC-type friction modifier on the wear performance of a hydrogenated DLC coating. *Wear*. 2013;302(s1-2):890. DOI: 10.1016/j.wear.2012.12.052
- [6] Moon K, Lee H, Sun S, Lee C, Shin S. Development and characterization of Zr-based multi-component nanocomposite coatings prepared using single alloying target. *Advanced Engineering Materials*. 2018;20(9):1700904. DOI: 10.1002/adem.201700904
- [7] Yoon H, Lee H, Shin S, Kwon S, Moon K. Preparation of Zr-Al-Mo-Cu single targets with glass forming ability and deposition of thin film metallic glass. *Coatings*. 2020;10(4):398. DOI: 10.3390/coatings10040398
- [8] Leyland A, Matthews A. Design criteria for wear-resistant nanostructured and glassy-metal coatings. *Surface and Coatings Technology*. 2004;177:317-324. DOI: 10.1016/j.surfcoat.2003.09.011
- [9] Hovsepian P, Lewis D, Munz W. Recent progress in large scale manufacturing of multilayer/superlattice hard coatings. *Surface and Coatings Technology*. 2000;133:166-175. DOI: 10.1016/S0257-8972(00)00959-2
- [10] Sigmund P. Theory of sputtering. I. Sputtering yield of amorphous and polycrystalline targets. *Physical Review Journals Archive*. 1969;184(2):383. DOI: 10.1103/PhysRev.184.383
- [11] Inoue A. Stabilization of metallic supercooled liquid and bulk amorphous alloys. *Acta Materialia*. 2000;48(1):279-306. DOI: 10.1016/S1359-6454(99)00300-6
- [12] Yoon H, Shin S, Kwon S, Moon K. Microstructure and mechanical properties of ZrCuSiN coatings deposited by a single alloy target. *Coatings*. 2020;10(5):435. DOI: 10.3390/coatings10050435
- [13] Debenedetti P, Stillinger F. Supercooled liquids and the glass transition. *Nature*. 2001;410(6825):259-267. DOI: 10.1038/35065704
- [14] Jung D, Lee C, Moon K. Nanocomposite Mo-Cu-N coatings deposited by reactive magnetron sputtering process with a single alloying target. *Ceramic Engineering and Science Proceedings*. 2014;34(3):89-96
- [15] Jung D, Moon K, Shin S, Lee C. Influence of ternary elements (X= Si, B, Cr) on TiAlN coating deposited by magnetron sputtering process with single alloying targets. *Thin Solid Films*.

2013;**546**:242-245. DOI: 10.1016/j.tsf.2013.05.046

[16] Fan C, Takeuchi A, Inoue A. Preparation and mechanical properties of Zr-based bulk Nanocrystalline alloys containing compound and amorphous phases. *Materials Transactions, JIM*. 1999;**40**(1):42-51. DOI: 10.2320/matertrans1989.40.42

[17] Yoon H, Choi J, Park H, Sun J, Shin S, Moon K. Zr-based thin-film metallic glass for bipolar plate in proton exchange membrane fuel cells. *Advanced Engineering Materials*. 2020;**22**(10):2000366. DOI: 10.1002/adem.202000369

[18] Erdemir A, Ramirez G, Eryilmaz O, Narayanan B, Liao Y, Kamath G, et al. Carbon-based tribofilms from lubricating oils. *Nature*. 2016;**536**(7614):67-71. DOI: 10.1038/nature18948

[19] Yoon H. Microstructural and Mechanical Properties of ZrCuSiN Thin Films Deposited by Reactive Magnetron Sputtering with Single Alloy Target [Thesis]. Pusan: Pusan National University; 2020

[20] Kim S, Yoon H, Moon K, Lee C. Mechanical and friction behavior of sputtered Mo-Cu-(N) coatings under various N₂ gas flow using a multicomponent single alloy target. *Surface and Coatings Technology*. 2021;**412**:127060. DOI: 10.1016/j.surfcoat.2021.127060

[21] Cha S-C, Park H-J, Lee J-H: Exploring the effectiveness of a complex coating technique for use the smallest parts of advanced powertrain fuel systems. *International Journal of Automotive Technology* 2020;**21**:667-673. DOI: 10.1007/s12239-020-0064-1

[22] CleanoSpector [Internet]. 2022. Available online: <https://www.sita-process.com/products/fluorescence-measuring-and-testing-devices/sita-cleanspector/> [Accessed: June 7, 2022]

[23] Recognoil [Internet]. 2022. Available online: https://www.recognoil.com/reco_en.html#about2W [Accessed: June 7, 2022]

[24] Joshi A. Review of vehicle engine efficiency and emissions. *SAE International Journal of Advances & Current Practices in Mobility*. 2020;**2**(5):2479-2507. DOI: 10.4271/2020-01-0352

[25] Park H, Cha S-C, Kim S. Development of new modified super saturated NitroCarburizing for modern high pressure injector. *SAE Technical Paper*. 2018;**2018**(01):1408. DOI: 10.4271/2018-01-1408

[26] Song Y, Kim J-H, Kim K-S, Kim S, Song PK. Effect of C₂H₂/H₂ gas mixture ratio in direct low-temperature vacuum carburization. *Metals*. 2018;**8**(7):493-505. DOI: 10.3390/met8070493

[27] Collins S, Williams P, Marx S, Heuer A, Ernst F, Kahn H. Low-temperature carburization of austenitic stainless steels. *ASM handbook, volume 4D. Heat Treating of Irons and Steels*. 2014;**4**(451):451-460. DOI: 10.31399/asm.hb.v04d.a0005939

[28] Ichii K, Fujimura K, Takase T. Structure of the ion-Nitrided layer of 18-8 stainless steel. *Technology Reports of Kansai University*. 1986;**27**:135-144 ISSN: 0453-2198

[29] Weiss B, Sticker R. Phase instabilities during high temperature exposure of 316 austenitic stainless steel. *Metallurgical and Materials Transactions B*. 1972;**4**:851-866. DOI: 10.1007/BF02647659

[30] Hummelshoj T. Mechanism of Metal Dusting Corrosion [Thesis].

DCAMM, Lyngby: Technical
University of Denmark; 2010. ISBN:
978-87-90416-28-7

[31] Dang J, Zhang G, Chou K,
Reddy R, Sun Y. Kinetics and mechanism
of hydrogen reduction of MoO₃ to MoO₂.
International Journal of Refractory
Metals and Hard Materials. 2013;**41**:216-
223. DOI: 10.1016/j.ijrmhm.2013.04.002

[32] De Micco G, Nassini H, Bohé A.
Kinetics of molybdenum oxidation
between 375 and 500°C. In: Saji V,
Lopatin S, editors. Molybdenum and its
Compounds. New York: Nova Science
Publishers. 2014. pp. 313-338. ISBN:
978-1-63321-210-7